Reactivity of Alkanes on Zeolites: A Computational Study of Propane Conversion Reactions

Xiaobo Zheng and Paul Blowers*

Department of Chemical and Environmental Engineering, The University of Arizona, P.O. Box 210011, Tucson, Arizona 85721-0011

Received: August 16, 2005; In Final Form: October 5, 2005

In this work, quantum chemical methods were used to study propane conversion reactions on zeolites; these reactions included protolytic cracking, primary hydrogen exchange, secondary hydrogen exchange, and dehydrogenation reactions. The reactants, products, and transition-state structures were optimized at the B3LYP/6-31G* level and the energies were calculated with CBS-QB3, a complete basis set composite energy method. The computed activation barriers were 62.1 and 62.6 kcal/mol for protolytic cracking through two different transition states, 30.4 kcal/mol for primary hydrogen exchange, 29.8 kcal/mol for secondary hydrogen exchange, and 76.7 kcal/mol for dehydrogenation reactions. The effects of basis set for the geometry optimization and zeolite acidity on the reaction barriers were also investigated. Adding extra polarization and diffuse functions for the geometry optimization did not affect the activation barriers obtained with the composite energy method. The largest difference in calculated activation barriers is within 1 kcal/mol. Reaction activation barriers do change as zeolite acidity changes, however. Linear relationships were found between activation barriers and zeolite deprotonation energies. Analytical expressions for each reaction were proposed so that accurate activation barriers can be obtained when using different zeolites as catalysts, as long as the deprotonation energies are first acquired.

1. Introduction

Zeolites are microporous crystalline aluminosilicates with three-dimensional framework structures which form uniformly sized pores of molecular dimension. They are broadly used as catalysts in the oil refining and petroleum industries; the worldwide total annual zeolite catalyst consumption rate was 360 million tons in 1998.[1] There are 130 different types of zeolite structures identified and described in the International Zeolite Association Database,[2] 16 of which are of commercial interest and are produced synthetically. Among them, H-ZSM-5 is broadly used in the petrochemical industry for catalytic cracking of hydrocarbons because of its interesting catalytic properties, including shape selectivity and high acid strength.[3]

The catalytic function of zeolites is realized by their Brønsted acidic sites. These active sites are formed when a silicon atom, which has a formal valency of four, is replaced by an aluminum atom with a valency of three. A proton is attached to the connecting oxygen atom between silicon and its aluminum neighbor, resulting in a chemically stable structure, Al(OH)Si, where the oxygen atom is in a three-coordinated structure. The SiO and AlO bonds are considerably covalent, creating a relatively weak OH bond. The "onium" type coordination of oxygen is the fundamental reason for the high acidity of the attached proton, which makes zeolites good catalysts.[4]

Because of complicated reaction mechanisms and various simultaneous reaction pathways, hydrocarbon catalytic reactions on zeolites are very difficult to study experimentally.[5,6] For propane reactions, only limited experimental information is available.[7−9] On the other hand, the increase in computer speed has greatly enabled application of computational tools in large systems in the past decade. Density functional theory and ab-initio quantum chemical methods have been applied by many researchers to study zeolite catalytic reactions quantitatively.[10−27] The results have led to a better understanding of the reaction mechanisms and kinetic and thermodynamic properties regarding these reactions.

The aspects of a catalytic reaction which are dependent only on local properties, such as the activation of adsorbates and any bond breaking or forming that may take place, generally can be studied with the cluster approach.[5,19,28] A cluster model is used to represent the catalyst, which is formed by cutting out a portion of the catalyst lattice and terminating the open valences with hydroxyl or hydride bonds. The cluster size is chosen so that the reaction can be modeled using quantum methods.[29] $H_3Si-O-AlH_2-(OH)-SiH_3$, a T3 cluster model, has been applied extensively to investigate hydrocarbon heterogeneous reactions,[30−34] which was also the cluster of choice to simulate the zeolite surface in this work.

In this work, density functional theory and ab-initio methods were implemented to investigate the four propane conversion reactions. The results were compared with experiment[7−9] and those from previous computational research.[14,32,35,36] Furthermore, the influence of the basis sets and zeolite acidity on the reaction activation barriers was studied quantitatively.

2. Computational Methods

All the calculations in this work were performed with the GAUSSIAN98 [37] software package, and all structures were obtained with Becke's three-parameter density functional[38] and the Lee, Yang, and Parr functional,[39] the well-known B3LYP method, with a moderate 6-31G* basis set. The energies were obtained with CBS-QB3, a high-level complete basis set

* Corresponding author. Tel.: 1-520-626-5319. Fax: 1-520-621-6048. E-mail: blowers@engr.arizona.edu.

10.1021/jp054605z CCC: $30.25
Published on Web 11/04/2005

composite energy method.[40] The products and reactants were verified with frequency calculations to be stable structures, and the transition states were tested to ensure they were first-order saddle points with only one negative eigenvalue. Additionally, intrinsic reaction coordinate (IRC) calculations[41] proved that each transition state linked the correct products with reactants. Zero-point vibrational energies (ZPVE) were obtained from harmonic vibrational frequencies calculated at the B3LYP/6-31G* level with a scaling factor of 0.9806.[42]

3. Results and Discussions

3.1. Protolytic Cracking Reaction. The protolytic cracking reaction

$$CH_3CH_2CH_3 + H_3SiOAlH_2(OH)SiH_3 \rightarrow CH_4 + H_3Si(OC_2H_5)AlH_2OSiH_3$$

consists of the C−C bond cleavage of propane by the zeolite Brønsted acid proton. The transition-state structure (TS1) calculated using the B3LYP/6-31G* method is shown in Figure 1a. This reaction is found to be similar to the protolytic cracking of ethane,[43] since it starts with a proton attaching to the C−C bond of propane. The acidic proton, H(14), attaches to the methyl group of the propane reactant, C(16), to form methane and a surface alkoxide product. In the transition-state structure, the acidic proton has been transferred to carbon C(16) and a methane molecule is almost formed. The left ethyl group of propane becomes a carbenium ion, $C_2H_5^+$, with a Mulliken charge of 0.51, and is bonded to the zeolite cluster. In the transition-state structure, the C(15)−C(16) structure stays in the same plane as the zeolite O(2)−Al(1)-O(3) plane and the C(15)−C(17) structure is perpendicular to the main zeolite cluster plane. The zeolite cluster plays an important role in this reaction. The right oxygen of the cluster, O(3), acts as a Brønsted acid which donates a proton, while the left oxygen, O(2), acts as a Lewis base which receives the ethyl group, demonstrating the bifunctional Brønsted acidic−Lewis basic nature of the zeolite catalyst.

The protolytic cracking reaction of propane is nearly thermoneutral with an activation barrier of 62.1 kcal/mol calculated with the CBS-QB3 method. The activation barrier obtained in this work is compared with the computational results from Rigby et al. in Table 1. The barrier obtained by Rigby using MP2/6-31G*//HF/3-21G (energy calculation method//geometry optimization method), 68.0 kcal/mol,[24] is much higher than the experimental result because MP2 energy calculations tend to overestimate barrier heights.[44−47] The experimental activation energies for the propane cracking reactions were reported to be 37.1 kcal/mol for the H-ZSM-5 zeolite and 39.5 kcal/mol for HY-M.[8,9] Our calculated activation barrier is also higher than the experimental value. The difference could be caused by the fact that the T3 cluster applied in this work is only a partial representation of the zeolite catalyst which does not include long-range interactions. Interestingly, Zygmunt recently studied the ethane protolytic cracking reaction with a T5 cluster.[13] The result obtained with MP2(fc)/6-31G*//MP2(fc)/6-31G* is even higher, 73.70 kcal/mol. The long-range correction obtained by the HF/6-31G* calculation for a 58T cluster model reduces the activation barrier by 14.50 kcal/mol. For the same scenario, long-range corrections could also lower our calculated barrier height and bring it much closer to the experimental value. The other reason for the high activation barrier obtained could be the moderate basis set 6-31G* used in the geometry optimization which will be tested in Section 3.4. Moreover, the zeolite acidic effect could also reduce our calculated activation barrier by 2 kcal/mol, which will be discussed in Section 3.5.

We found another transition state (TS2) for the protolytic reaction and it is depicted in Figure 1b. In this transition state, the C(17)−C(15)−C(16) plane becomes perpendicular to the main zeolite cluster plane O(2)−Al(1)−O(3). Considering the cluster is only one part of the zeolite pore, this transition-state structure represents the case where the propane molecule is perpendicular to the plane of the zeolite pores. This mechanism becomes more important when the reactant hydrocarbon chain length becomes larger. For zeolites with small to medium pores, like ZSM-5 which is broadly used for hydrocarbon cracking, the reactant molecule becomes comparable to the zeolite pore diameter for those species with a contiguous carbon chain length larger than three. The species become too large to pass in a parallel manner through the pores. As a result, the reaction can take place only when the reactant molecules are perpendicular to the zeolite pores. In other words, starting with a carbon chain length of four, like *n*-butane as a reactant, the perpendicular transition state is the only reaction pathway for the protolytic cracking reaction.

The activation barrier of this protolytic cracking pathway is 62.6 kcal/mol calculated with the CBS-QB3 method. The barrier is similar to that of TS1, 62.1 kcal/mol, which indicates that the two competitive reaction pathways are comparable. Again, this activation barrier is higher than that obtained by experiment.[9]

3.2. Hydrogen Exchange Reactions. The propane hydrogen exchange reaction can take place at either the primary carbon or the secondary carbon shown in the following reaction scheme:

$$CH_3CH_2\underline{\mathbf{C}}H_3 + H_3SiOAlH_2(OH')SiH_3 \rightarrow CH_3CH_2\underline{\mathbf{C}}H_2H' + H_3Si(OH)AlH_2OSiH_3$$

$$CH_3\underline{\mathbf{C}}H_2CH_3 + H_3SiOAlH_2(OH')SiH_3 \rightarrow CH_3\underline{\mathbf{C}}HH'CH_3 + H_3Si(OH)AlH_2OSiH_3$$

The bold underlined carbon atom indicates the place where hydrogen exchange takes place. The propane hydrogen exchange reactions were previously studied by this group[30] and are briefly discussed here for completeness of this work. Figure 1c shows the calculated transition-state structure for the primary hydrogen exchange reaction of propane using the B3LYP/6-31G* method. The structure clearly shows the C_s symmetry obtained without any symmetry constraints applied for the optimization step. The carbon in the main plane of the zeolite structure, C(15), is protonated and becomes a pentacoordinated structure. The exchanging hydrogen atom from propane, H(19), and the acidic proton, H(14), stay in the middle of the carbon and two oxygen atoms, indicating formation of one C−H bond and breaking of the other.

The activation barrier obtained with the CBS-QB3 method is 30.4 kcal/mol. In Table 1, the activation barrier is compared with previous computational results from Esteves[36] and Ryder.[35] The activation barrier obtained in this work is relatively lower than the calculated results from Esteves and Ryder which are 32.2 and 40.5 kcal/mol, respectively. The experimental activation energy reported by Stepanov et al. is 25.8 ± 1.7 kcal/mol.[7] Our calculation is only 3 kcal/mol higher than the maximum experimental data and is much closer to the experiment than those from Esteves and Ryder.

The calculated transition-state structure of propane secondary hydrogen exchange with the B3LYP method is shown in Figure 1d. The propane structure tilts to the right side of the zeolite

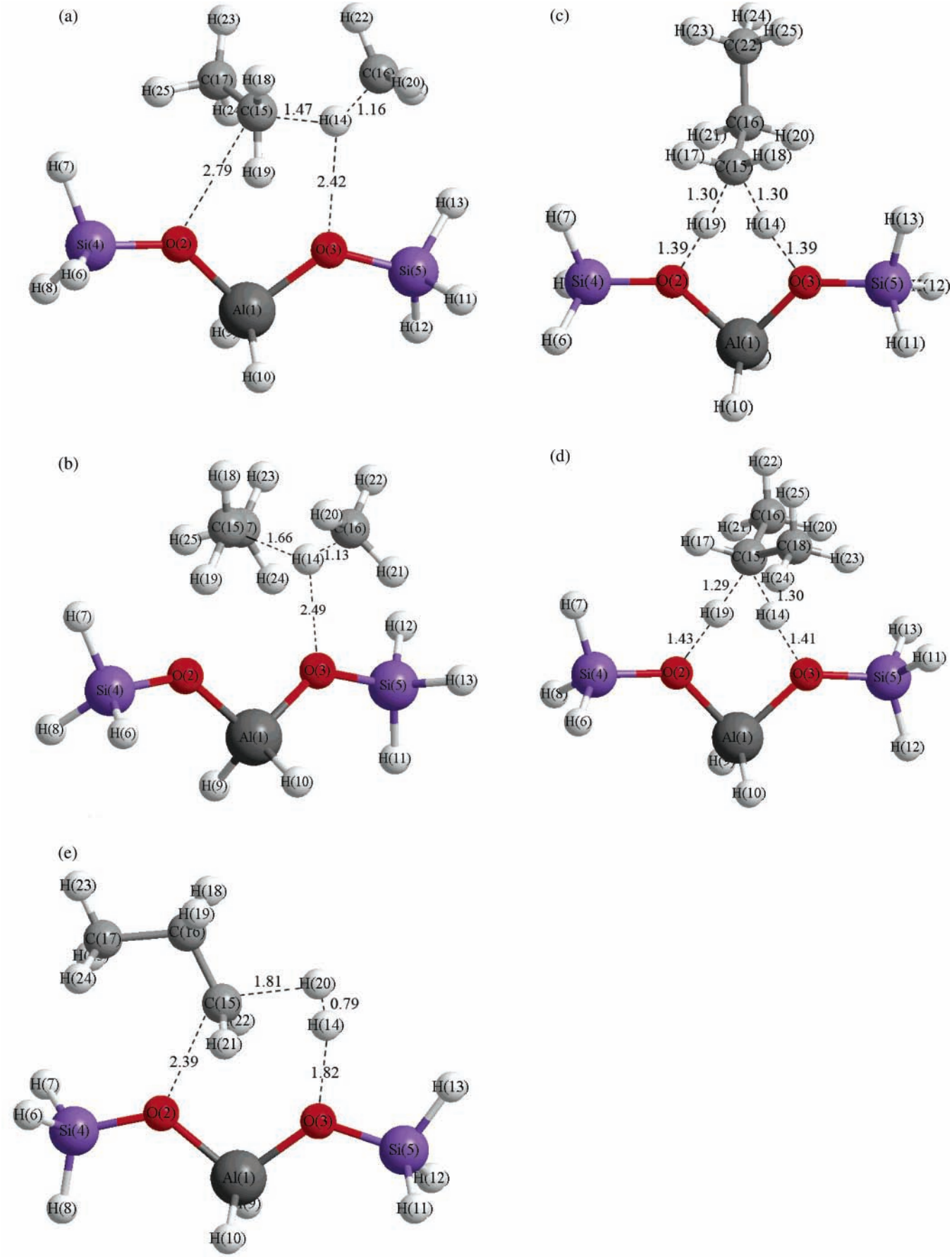

Figure 1. Transition-state structures for propane reactions on zeolite cluster (a) cracking reaction (TS1), (b) cracking reaction (TS2), (c) primary hydrogen exchange reaction, (d) secondary hydrogen exchange reaction, and (e) dehydrogenation reaction (units in Å).

TABLE 1: Activation Barrier Calculation Results for Propane Conversion Reactions on Zeolites Using the CBS Method (units in kcal/mol)

	computational results					experiment		
	This Work	Rigby[b]	Furtado[c]	Esteves[d]	Ryder[e]	Narbeshuber[f]		Stepanov[g]
cluster model/ catalyst type	T3	T3	T5	T3	T5	H-ZSM-5	HY-M	H-ZSM-5
geometry opt. method	B3LYP /6-31G*	HF /3-21G	B3LYP / 6-311G**	B3LYP / 6-31G**	BH&HLYP / 6-31++G **			
energy calculation method	CBS-QB3	MP2 /6-31G*	B3LYP / 6-311G**	B3LYP / 6-31G**	BH&HLYP / 6-31++G **			
cracking	(62.1/ 62.6)[a]	68.0				37.1	39.5	
primary hydrogen Exchange	30.4			32.2	40.5			25.8 ± 1.7
secondary hydrogen exchange	29.8			33.3	39.2			28.0 ± 1.7
dehydrogenation	76.7		73.0			22.7	15.6	

[a] (TS1/TS2). [b] Ref 14. [c] Ref 32. [d] Ref 36. [e] Ref 35. [f] Refs 8,9. [g] Ref 7.

TABLE 2: Calculated Activation Barriers for the Propane Protolytic Cracking Reaction with Different Basis Sets

geometry opt. method	cracking (TS1)	cracking (TS2)	primary hydrogen exchange	secondary hydrogen exchange	dehydrogenation
B3LYP/6-31G*	62.1	62.6	30.4	29.8	76.7
B3LYP/6-31G**	62.1	62.6	30.5	29.9	76.1
B3LYP/6-31++G**	62.3	62.6	30.6	30.1	75.8

cluster and pushes the acidic proton, H(14), farther away from the C(15) atom. As a result, the C(15)−H(14) distance is slightly larger than the C(15)−H(19) distance, while the distance of H(14)−O(3) is slightly less than that of H(19)−O(2). The activation barrier obtained with the CBS-QB3 method is 29.8 kcal/mol, which is very similar to the activation barrier for the primary hydrogen exchange reaction. The result is again much lower than the calculated results from Esteves and Ryder, which are 33.3 and 39.2 kcal/mol as listed in Table 1. Compared with the experimental activation energy of 28.0 ± 1.7 kcal/mol,[7] our calculated result falls within the experimental error range. Our calculated results show that the activation barrier of the secondary carbon−hydrogen exchange reaction is close to, but relatively lower than, that of primary carbon. This trend is the same as that obtained by Ryder,[35] but contradictory to the experimental results of Stepanov.[7] Since the experimental activation energy of primary and secondary exchange reactions only differs by 2.2 kcal/mol, the relative magnitude of these two activation energies could be reversed considering the experimental error range is as large as ±1.7 kcal/mol for each reaction. Also, because the difference of our calculational results is less than 1 kcal/mol and the accuracy of CBS composite energy calculations is around 1 kcal/mol, the relative magnitude of the our calculated activation barriers could be reversed to match the experiments listed here.

3.3. Dehydrogenation Reaction. The dehydrogenation reaction consists of cleavage of a C−H bond by the zeolite Brønsted acid proton.

$$CH_3CH_2CH_3 + H_3SiOAlH_2(OH)SiH_3 \rightarrow H_2 + H_3Si(OC_3H_7)AlH_2OSiH_3$$

The transition-state structure of the propane dehydrogenation reaction is shown in Figure 1e. The carbon C(15) structure becomes almost planar, and the other two carbons keep the tetrahedral structure. A six-member ring, O(2)−Al(1)−O(3)−H(14)−H(20)−C(15), is formed. With the H(20)−C(15) and H(14)−O(3) distances greatly extended to 1.81 and 1.82 Å, a di-hydrogen molecule, H(14)H(20), is almost formed, whereas the C_3H_7 fragment binds to the zeolite oxygen, O(2), which acts as a Lewis base.

The activation barrier obtained with the CBS-QB3 method is 76.7 kcal/mol. This barrier is the highest among all of the propane conversion reactions, indicating it is the most difficult reaction to take place. Our result is 3.7 kcal/mol higher than the result obtained by Furtado et al. [32] using B3LYP/6-311G**// B3LYP/6-31G**. However, B3LYP energy calculation methods have been well-known for underestimation of activation barriers.[6,48−50] The experimental study from Narbeshuber et al. reported activation energies of 22.7 and 15.5 kcal/mol for H-ZSM-5 and H-Y zeolites.[9] It seems clear that the computational results are too high compared to these experimental values, which is similar to the propane cracking reaction from Section 3.1. This discrepancy could be attributed to the relatively small cluster size and basis set choice for the optimization. Furtado increased the cluster size to T5 and used a larger basis set to refine their results. However, the activation barriers obtained increased by 3 kcal/mol, which could eliminate the doubt of the choice of the cluster size and basis set.

Interestingly, Kanzansky found another two-step reaction pathway for the isobutane dehydrogenation reaction.[51] But the activation barrier obtained was similar to that of the single-step pathway, which is still much higher than the experimental data. However, from previous experimental studies, the overall heat of reaction for the gas-phase dehydrogenation reaction $C_3H_8 \rightarrow C_3H_6 + H_2$ is known to be about 30 kcal/mol, which is difficult to reconcile with the reported experimental barriers.[5] Certainly, some discrepancy is caused by the failure of density functional theory to account for van der Waals interactions. But it is also possible that the experimental value is too low, considering the gas-phase heat of reaction value.

3.4. Basis Set Effects. In this work, the moderate 6-31G* basis set used in the geometry optimizations may seem inadequate. Therefore, the influence of the basis set on the activation barriers was investigated by increasing the basis set from 6-31G* to 6-31G** and 6-31++G** for the geometry optimization. The energies were then obtained using the composite CBS-QB3 method. As shown in Table 2, there is little difference between the activation barriers obtained using these three basis sets. The largest difference is for the dehydrogenation reaction where the activation barrier is reduced by less than 1 kcal/mol. Therefore, the diffuse and polarization functions added do not obtain better activation barriers with higher-level calculated energies. This proves that the calculated activation barriers depend greatly on the level of the energy calculation method and depend less on

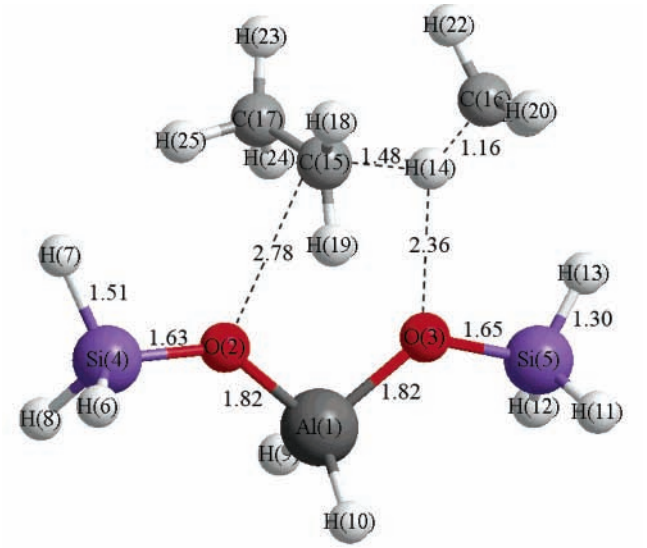

(a) R_{Si-H} = 1.3 Å (less acidic)

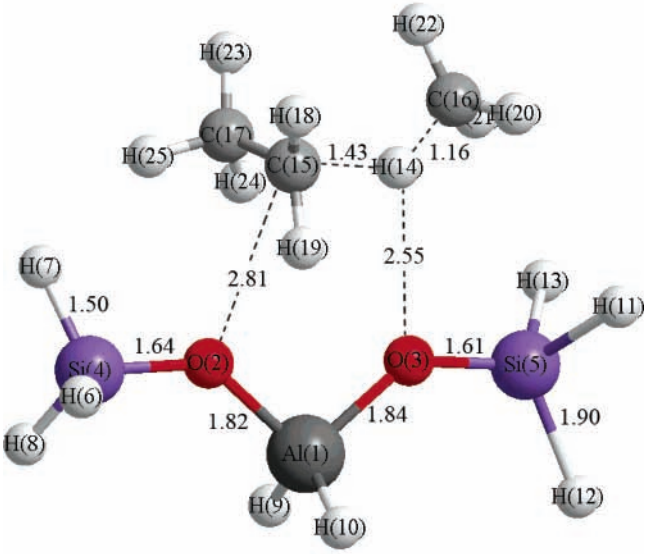

(b) R_{Si-H} = 1.9 Å (more acidic)

Figure 2. Transition-state structures of propane cracking reaction with changing terminal Si−H bond distances (units in Å).

the level of the geometry optimization method.[19,43] Using high-level calculations to obtain the activation barriers through the CBS-QB3 method is crucial in this situation. Therefore, the geometry optimized using the 6-31G* basis set is adequate for activation barriers as long as the final energy is obtained using a high-level method like CBS-QB3.

3.5. Acidity Effects. The acidity study of zeolite catalysts is important since the catalytic activity of zeolites is directly related to the strength of the acid sites.[52] The deprotonation energy (E_{dep}) of zeolite clusters is a theoretical measurement of zeolite acidity and is a good indicator of its chemical properties.[52−57] It is defined as the energy difference between the protonated (ZH) and unprotonated (Z^-) clusters.[54]

$$E_{dep} = E(Z^-) - E(ZH)$$

A high deprotonation energy indicates a stronger bond between the acidic hydrogen and its oxygen neighbor, which is also referred to as a being less acidic. Therefore, it takes more

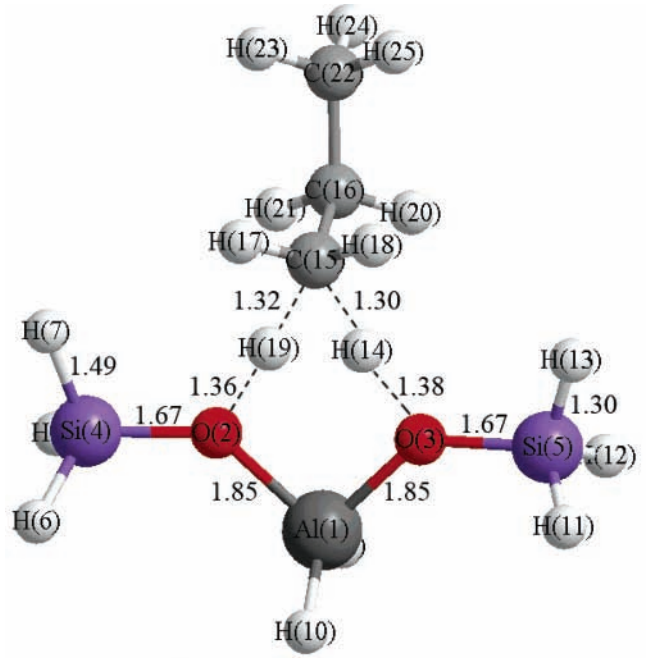

(a) R_{Si-H} = 1.3 Å (less acidic)

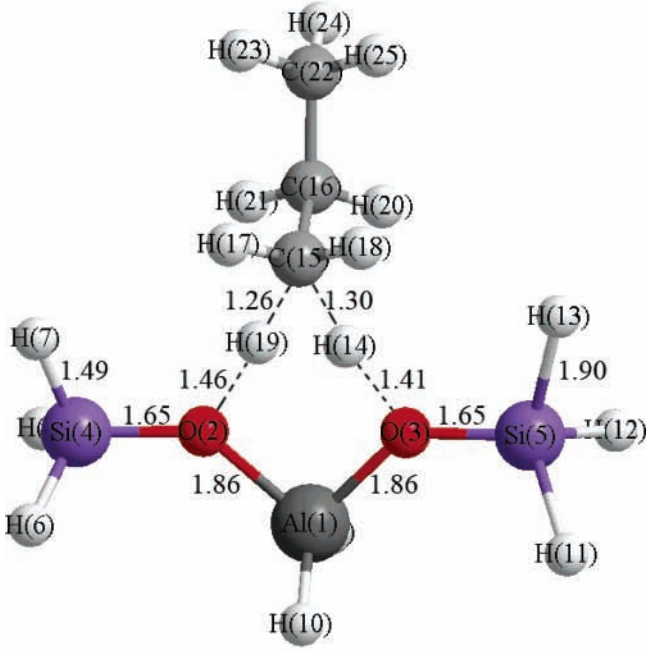

(b) R_{Si-H} = 1.9 Å (more acidic)

Figure 3. Transition-state structures of propane primary hydrogen exchange reaction with changing terminal Si−H bond distances (units in Å).

energy to break the H−O bond so that the reaction can take place, which means a higher activation barrier. In real zeolite catalysts, the deprotonation energy varies over a range of 20−50 kcal/mol among different zeolite structures.[6,58] For H-ZSM-5, the deprotonation energy has been studied by several researchers, and the numbers are in the range of 280−320 kcal/mol.[52−57,59] The corrected deprotonation energy of 295.4 kcal/mol[53] has now been extensively accepted for H-ZSM-5 zeolite.[13,19,43]

Kramer et al.[60] have shown that the acidity effect of zeolite catalysts can be simulated by modifying the length of the

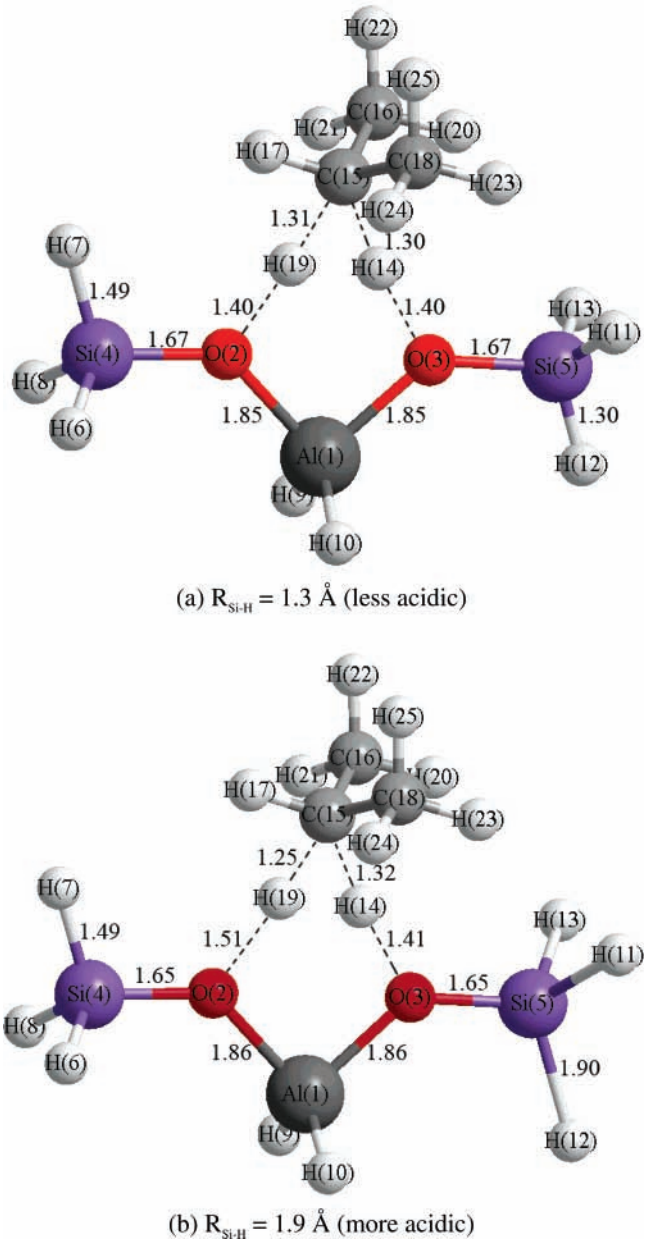

Figure 4. Transition-state structures of propane secondary hydrogen exchange reaction with changing terminal Si−H bond distances (units in Å).

terminal Si−H bonds of the cluster model with all other geometry parameters fully optimized, and our previous work has followed this methodology.[31] With the increase of the terminal Si−H bond distance, the zeolite cluster acidity increases and its deprotonation energy decreases. The changes of the zeolite acidity affect the transition-state structures and activation barriers of the reactions. Figure 2 shows the transition-state structures of the propane protolytic cracking reaction as the Si−H distance changes from 1.3 to 1.9 Å. With a Si−H bond length increase, the distance of the protonic hydrogen and acidic oxygen, H(14)−O(3), increases from 2.36 to 2.55 Å. Similarly, the distance between the carbon atom and Lewis basic oxygen, C(15)−O(2), increases from 2.78 to 2.81 Å. The C_3H_9 group moves farther away from the cluster, while the two cracking carbon atoms, C(15) and C(16), move closer. Additionally, the oxygen and silicon distance, O(3)−Si(5), shrinks as the cluster acidity increases, indicating a stronger O−Si bond, which in turn causes a weak oxygen bond to the acidic proton.

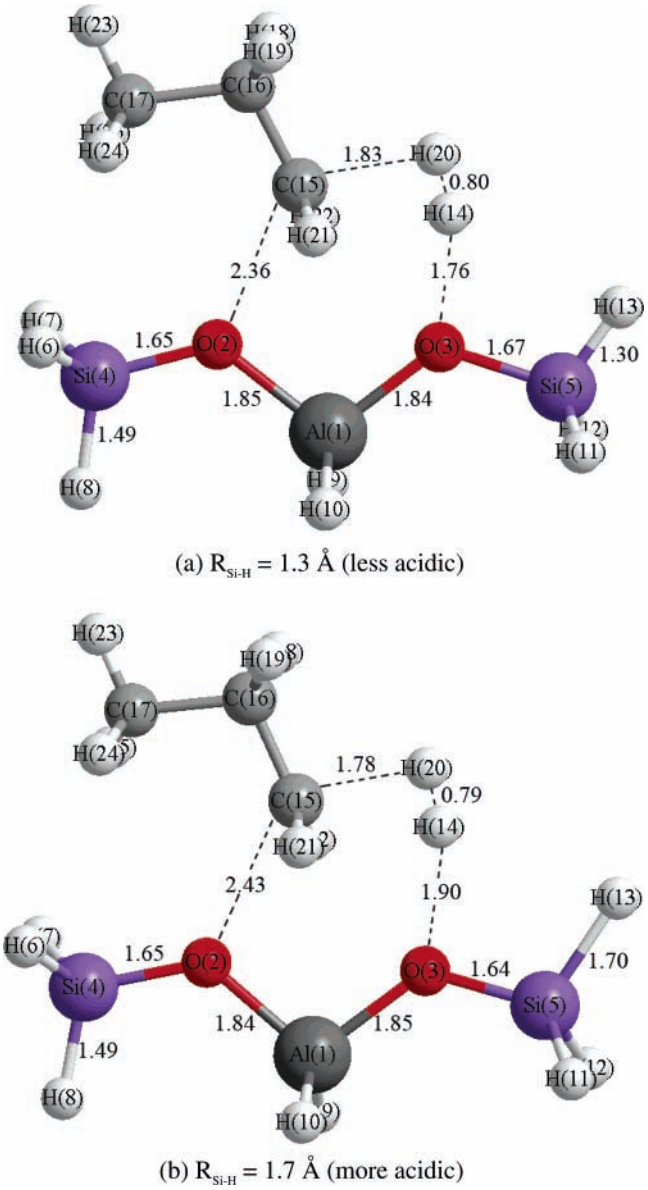

Figure 5. Transition-state structures of propane dehydrogenation reaction with changing terminal Si−H bond distances (units in Å).

Similar acidic effects were studied and applied to propane primary and secondary hydrogen exchange reactions shown in Figures 3 and 4. As the cluster acidity increases, the acidic hydrogen and oxygen distance, H(14)−O(3), increases. Meanwhile, the C_3H_9 structure moves away from the zeolite cluster, which is similar to protolytic cracking and secondary hydrogen exchange reactions. However, a transition state cannot be located for the propane dehydrogenation reaction as the Si−H distance increases to 1.9 Å. The transition-state structures of the propane dehydrogenation reaction as the Si−H distance changes to 1.3 and 1.7 Å are shown in Figure 5. As the Si−H distance increases, the distance of the carbon atom and Lewis basic oxygen, C(15)−O(2), increases from 2.36 to 2.43 Å and the distance of protonic hydrogen and acidic oxygen, H(14)−O(3), increases from 1.76 to 1.90 Å. Meanwhile, the bi-hydrogen atoms, H(14) and H(20), move closer to each other, becoming more like the structure of a hydrogen molecule, and the entire C_3H_9 group moves farther away from the cluster.

Table 3 summarizes the change in activation barriers for propane protolytic cracking, primary and secondary hydrogen exchange, and dehydrogenation reactions as the Si−H bond

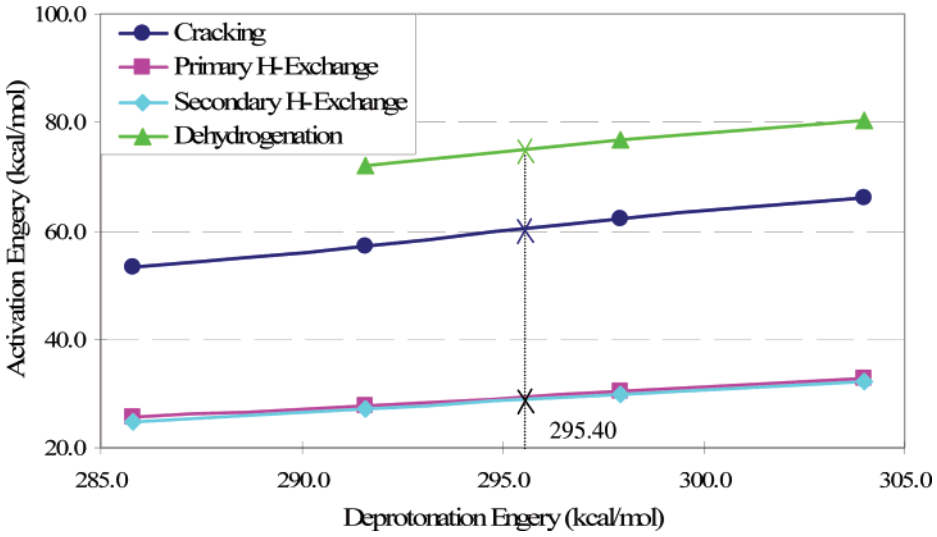

Figure 6. Corrections to the calculated propane conversion reactions activation barriers for the acidity effect.

TABLE 3: Effects of Si−H Distances on Activation Barriers (units in kcal/mol)

	activation barrier (E_a)				
	protolytic cracking	primary hydrogen exchange	secondary hydrogenexchange	dehydrogenation	deprotonation energy (E_{dep})
R_{Si}−H = 1.30 Å	66.1	32.8	32.2	80.5	304.0
R_{Si}−H = 1.47 Å	62.1	30.4	29.8	76.7	297.9
R_{Si}−H = 1.70 Å	57.3	27.7	27.0	72.0	291.6
R_{Si}−H = 1.90 Å	53.4	25.6	24.9	N/A	285.8
H-ZSM-5 zeolite	60.1	29.4	28.7	74.7	295.4
expression	$E_a = 0.708E_{dep} - 148.9$	$E_a = 0.396E_{dep} - 87.6$	$E_a = 0.405E_{dep} - 90.8$	$E_a = 0.686E_{dep} - 127.9$	

distances are varied. With the Si−H distance increasing, the activation barriers decrease for all four reactions because of the increased acidity of the zeolite cluster. As long as the reaction mechanism does not alter, the change in activation barrier is linearly correlated to the change in zeolite cluster deprotonation energy. Therefore, the Brønsted−Polanyi principle can be applied:[61]

$$\Delta E_a = c\Delta E_{dep} \text{ or } E_a = c\Delta E_{dep} + b$$

The linear relationship of the activation barriers with cluster deprotonation energies is illustrated in Figure 6. Applying the H-ZSM-5 zeolite catalyst deprotonation energy, 295.4 kcal/mol,[53] the activation barriers are then calculated and listed in Table 3. For the propane protolytic cracking reaction, the activation barrier obtained is 60.1 kcal/mol using the expression $E_a = 0.708E_{dep} - 148.9$. Therefore, with the acidity effect correction, the barrier height is reduced by 2.0 kcal/mol. Similarly, the barrier heights were lowered by 1.0, 1.1, and 2.0 kcal/mol for primary hydrogen exchange, secondary hydrogen exchange, and dehydrogenation reactions, respectively, which brings our computational results even closer to the experimental results.

The acidity effect study has shown the correlation between the zeolite deprotonation energy and activation barrier for propane conversion reactions. This is crucial because zeolite deprotonation energies are significantly easier to calculate than activation barriers because of the difficulty in performing transition-state optimizations for large complexes with many degrees of freedom. Applying these analytical expressions, activation barriers can be obtained for different zeolite catalysts as long as their deprotonation energies are first acquired.

Conclusions

In this work, propane protolytic cracking, primary hydrogen exchange, secondary hydrogen exchange, and dehydrogenation reactions catalyzed by a zeolite cluster were studied using a T3 cluster. The transition-state structures were optimized using the B3LYP method, and the energies were obtained using CBS-QB3, a complete basis set composite energy method. The effects of basis set on the activation barriers were investigated. The increase of basis set for the geometry optimization proved to have negligible effects on the reaction barrier heights.

The activation barriers obtained for cracking, primary and secondary hydrogen exchange, and dehydrogenation reactions are 62.1, 62.6, 30.4, 29.8, and 76.7 kcal/mol, respectively. This indicates that the hydrogen exchange reaction has the lowest barrier and is the easiest reaction to take place, while the dehydrogenation reaction has the highest barrier and is the most difficult to happen. Furthermore, the zeolite acidity effect was mimicked by changing the terminating Si−H bond lengths. Analytic relationships between the activation barriers and deprotonation energies were proposed so that accurate reaction barriers can be obtained when using zeolite catalysts with different acidities.

Acknowledgment. This work was funded by the State of Arizona through the Office of the Vice President for Research at the University of Arizona. Supercomputer time was provided by the National Computational Science Alliance and used the NCSA HP/ Convex Exemplar SPP-2000 at the University of Illinois at Urbana-Champaign. Part of the supercomputer time was provided by National Partnership for Advanced Computational Infrastructure and used the IBM pSeries 690 and pSeries 655 at Boston University.

References and Notes

(1) Maesen, T.; Marcus, B. *Studies in Surface Science and Catalysis* **2001**, *137* (*Introduction to Zeolite Science and Practice* (*2nd ed.*)), 1.
(2) http://www.iza-structure.org/databases/.

(3) McCusker, L. B.; Baerlocher, C. *Studies in Surface Science and Catalysis* **2001**, *137* (*Introduction to Zeolite Science and Practice* (*2nd ed.*)), 37.

(4) Flanigen, E. M. *Studies in Surface Science and Catalysis* **2001**, *137* (*Introduction to Zeolite Science and Practice* (*2nd ed.*)), 11.

(5) Curtiss, L. A.; Gordon, M. S. *Computational materials chemistry methods and applications*; Kluwer Academic Publishers: Dordrecht, Boston, London, 2004.

(6) vanSanten, R. A.; van de Graaf, B.; Smit, B. *Studies in Surface Science and Catalysis* **2001**, *137* (*Introduction to Zeolite Science and Practice* (*2nd ed.*)), 419.

(7) Stepanov, A. G.; Ernst, H.; Freude, D. *Catal. Lett.* **1998**, *54*, 1.

(8) Narbeshuber, T. F.; Vinek, H.; Lercher, J. A. *J. Catal.* **1995**, *157*, 388.

(9) Narbeshuber, T. F.; Brait, A.; Seshan, K.; Lercher, J. A. *J. Catal.* **1997**, *172*, 127.

(10) Blaszkowski, S. R.; Jansen, A. P. J.; Nascimento, M. A. C.; vanSanten, R. A. *J. Phys. Chem.* **1994**, *98*, 12938.

(11) Blaszkowski, S. R.; Nascimento, M. A. C.; vanSanten, R. A. *J. Phys. Chem.* **1996**, *100*, 3463.

(12) Hay, P. J.; Redondo, A.; Guo, Y. J. *Catal. Today* **1999**, *50*, 517.

(13) Zygmunt, S. A.; Curtiss, L. A.; Zapol, P.; Iton, L. E. *J. Phys. Chem. B* **2000**, *104*, 1944.

(14) Rigby, A. M.; Kramer, G. J.; vanSanten, R. A. *J. Catal.* **1997**, *170*, 1.

(15) Collins, S. J.; Omalley, P. J. *J. Catal.* **1995**, *153*, 94.

(16) Frash, M. V.; Kazansky, V. B.; Rigby, A. M.; vanSanten, R. A. *J. Phys. Chem. B* **1998**, *102*, 2232.

(17) Himei, H.; Yamadaya, M.; Kubo, M.; Vetrivel, R.; Broclawik, E.; Miyamoto, A. *J. Phys. Chem.* **1995**, *99*, 12461.

(18) Kazansky, V. B.; Frash, M. V.; vanSanten, R. A. *Appl. Catal*., *A*: *General* **1996**, *146*, 225.

(19) Frash, M. V.; vanSanten, R. A. *Top. Catal.* **1999**, *9*, 191.

(20) Kazansky, V. B. *Catal. Today* **1999**, *51*, 419.

(21) Kazansky, V. B.; Frash, M. V.; vanSanten, R. A. Quantum-chemical study of the nonclassical carbonium ion-like transition states in isobutane cracking on zeolites. In *11th International Congress on Catalysis*—40th Anniversary, Parts A and B **1996**, *101*, 1233.

(22) Collins, S. J.; Omalley, P. J. *Chem. Phys. Lett.* **1994**, *228*, 246.

(23) Viruelamartin, P.; Zicovichwilson, C. M.; Corma, A. *J. Phys. Chem.* **1993**, *97*, 13713.

(24) Kazansky, V. B.; Senchenya, I. N.; Frash, M.; vanSanten, R. A. *Catal. Lett.* **1994**, *27*, 345.

(25) Kazansky, V. B.; Frash, M. V.; vanSanten, R. A. *Catal. Lett.* **1994**, *28*, 211.

(26) Rigby, A. M.; Frash, M. V. *J. Mol. Catal*., *A*—Chem. **1997**, *126*, 61.

(27) Klier, K. *Top. Catal.* **2002**, *18*, 141.

(28) Neurock, M. *J. Catal.* **2003**, *216*, 73.

(29) Bates, S. P.; vanSanten, R. A. *Adv. Catal.* **1998**, *42*, 1.

(30) Zheng, X.; Blowers, P. *J. Phys. Chem. A,* submitted.

(31) Zheng, X.; Blowers, P. *J. Mol. Catal. A* **2005**, *229*, 77.

(32) Furtado, E. A.; Milas, I.; Lins, J.; Nascimento, M. A. C. *Phys. Status Solidi A* **2001**, *187*, 275.

(33) Okulik, N. B.; Diez, R. P.; Jubert, A. H.; Esteves, P. M.; Mota, C. J. A. *J. Phys. Chem. A* **2001**, *105*, 7079.

(34) Okulik, N. B.; Diez, R. P.; Jubert, A. H. *J. Phys. Chem. A* **2004**, *108*, 2469.

(35) Ryder, J. A.; Chakraborty, A. K.; Bell, A. T. *J. Phys. Chem. B* **2000**, *104*, 6998.

(36) Esteves, P. M.; Nascimento, M. A. C.; Mota, C. J. A. *J. Phys. Chem. B* **1999**, *103*, 10417.

(37) Frisch, M. J.; Trucks, G. W.; Schlegel, H. B.; Gill, P. M. W.; Johnson, B. G.; Robb, M. A.; Cheeseman, J. R.; Keith, T.; Petersson, G. A.; Montgomery, J. A.; Raghavachari, K.; Al-Laham, M. A.; Zakrzewski, V. G.; Ortiz, J. V.; Foresman, J. B.; Cioslowski, J.; Stefanov, B. B.; Nanayakkara, A.; Challacombe, M.; Peng, C. Y.; Ayala, P. Y.; Chen, W.; Wong, M. W.; Andres, J. L.; Replogle, E. S.; Gomperts, R.; Martin, R. L.; Fox, D. J.; Binkley, J. S.; Defrees, D. J.; Baker, J.; Stewart, J. P.; Head-Gordon, M.; Gonzalez, C.; Pople, J. A. *Gaussian98*, Revision A.7; Gaussian, Inc.: Pittsburgh, PA, 1995.

(38) Becke, A. D. *J. Chem. Phys.* **1993**, *98*, 5648.

(39) Lee, C. T.; Yang, W. T.; Parr, R. G. *Phys. Rev. B* **1988**, *37*, 785.

(40) Montgomery, J. A.; Frisch, M. J.; Ochterski, J. W.; Petersson, G. A. *J. Chem. Phys.* **1999**, *110*, 2822.

(41) Gonzalez, C.; Schlegel, H. B. *J. Chem. Phys.* **1989**, *90*, 2154.

(42) Scott, A. P.; Radom, L. *J. Phys. Chem.* **1996**, *100*, 16502.

(43) Zheng, X. B.; Blowers, P. *J. Mol. Catal. A*—Chem. **2005**, *229*, 77.

(44) Willis, B. G.; Jensen, K. F. *J. Phys. Chem. A* **1998**, *102*, 2613.

(45) Lee, W. T.; Masel, R. I. *J. Phys. Chem.* **1996**, *100*, 10945.

(46) Lee, W. T.; Masel, R. I. *J. Phys. Chem.* **1995**, *99*, 9363.

(47) Yamataka, H.; Nagase, S.; Ando, T.; Hanafusa, T. *J. Am. Chem. Soc.* **1986**, *108*, 601.

(48) Truong, T. N. *J. Chem. Phys.* **2000**, *113*, 4957.

(49) Lynch, B. J.; Truhlar, D. G. *J. Phys. Chem. A* **2001**, *105*, 2936.

(50) Goldstein, E.; Haught, M.; Tang, Y. *J. Comput. Chem.* **1998**, *19*, 154.

(51) Kazansky, V. B.; Frash, M. V.; vanSanten, R. A. *Appl. Catal*., *A*: *Gen.* **1996**, *146*, 225.

(52) Sillar, K.; Burk, P. *J. Mol. Struct.*—Theochem **2002**, *589*, 281.

(53) Sauer, J.; Sierka, M. *J. Comput. Chem.* **2000**, *21*, 1470.

(54) Brand, H. V.; Curtiss, L. A.; Iton, L. E. *J. Phys. Chem.* **1993**, *97*, 12773.

(55) Eichler, U.; Brandle, M.; Sauer, J. *J. Phys. Chem. B* **1997**, *101*, 10035.

(56) Datka, J.; Boczar, M.; Rymarowicz, P. *J. Catal.* **1988**, *114*, 368.

(57) Grau-Crespo, R.; Peralta, A. G.; Ruiz-Salvador, A. R.; Gomez, A.; Lopez-Cordero, R. *Phys. Chem. Chem. Phys.* **2000**, *2*, 5716.

(58) vanSanten, R. A.; De Bruyn, D. P.; Den Ouden, C. J. J.; Smit, B. *Studies in Surface Science and Catalysis* **1991**, *58* (*Introduction to Zeolite Science and Practice*), 317.

(59) Sillar, K.; Burk, P. *J. Phys. Chem. B* **2004**, *108*, 9893.

(60) Kramer, G. J.; Vansanten, R. A.; Emeis, C. A.; Nowak, A. K. *Nature* **1993**, *363*, 529.

(61) vanSanten, R. A.; Niemantsverdriet, J. W. *Chemical kinetics and catalysis*; Plenum Press: New York, 1995.